Modelling and Simulation in Materials Science and Engineering

A Model and simulation of lattice vibrations in a superabundant vacancy phase of palladium-deuterium

To cite this article before publication: M. R. Staker 2020 *Modelling Simul. Mater. Sci. Eng.* in press https://doi.org/10.1088/1361-651X/ab9994

In preparation for Mod. Sim. in Mat. Sci & Engr 28. (2020) xx–xx

A Model and simulation of lattice vibrations in a superabundant vacancy phase of palladium-deuterium

M. R. Staker [a, b, *]

[a] *Department of Engineering, Loyola University Maryland, 4501 North Charles St, Baltimore, MD, 21210, USA*
[b] *American Patent Institute, 2817 Wesleyan Drive, Churchville, MD 21028, USA*
* *E-mail:* m.r.staker@alum.mit.edu (best) or mstaker@loyola.edu

ABSTRACT

A one dimensional Bravais lattice model is applied to a superabundant vacancy (SAV) delta δ phase (Pd_3VacD_4 - octahedral), in the palladium – deuterium system. SolidWorks is used to simulate the motion of atoms and ions in the lattice. These two approaches give identical results for the vibrations of the deuterons indicating that large vibrations of deuterons are possible when the microstructure is a mixture of beta deuteride and small volume percent delta SAV phase. These conditions result from the unique geometry and crystallography of δ phase. According to both the model and simulation, as the size of δ phase increases, opportunity for high amplitude vibrations of deuterons increases. Increasing temperature should have a similar effect.

Keywords: Superabundant vacancy structures, Palladium - Isotopic Hydrogen phases, Delta δ and Delta Prime δ′ Phases, Lattice Vibrations, Resonance Frequency, Phonons

1. Introduction

Superabundant vacancy phases (SAV) offer unique crystallography because the high levels of vacancies (~ 25%) are ordered [1-21]. In the ordered Pd_3VacD_4 SAV phase, Deuterium (D) occupies octahedral interstitial sites of the palladium (Pd) face centered cubic structure (FCC) as positive deuterons (D^+), and vacancies (Vac^-) occupying all unit cell corners with some negative charge. This phase, called delta (δ) phase, is located on the Pd-D phase diagram [22, 23] at a nominal D/Pd ratio of 1.33. The unique feature is orthogonal empty channels, along contiguous unit cell edges, <100> directions, occupied only by regularly spaced deuterons with spacing equal to the unit cell lattice parameter. If the deuterons migrate to tetrahedral interstitial sites [24-26], the SAV phase is δ′ [22, 23], with empty channels or vacancy tubes with apparent enhanced electronic conduction [23]. In either case, diameters of these tubes vary periodically when traversing <100> directions along contiguous unit cells. Its diameter ranges from a minimum of .414 of the Pd atom at the edge midpoint of the FCC unit cell (octahedral position), to a maximum value of the diameter of the Pd atom at corners of the unit cell [23]. Ignoring hydrogen, invisible to X-rays, and with ordered Vac^-, the unit cell of SAV phases is simple cubic (SC).

The properties of the SAV phases are not well known except: 1) the crystallography from X-ray diffraction, 2) unit cell dimensional behavior (contraction upon formation from the beta (β) deuteride or hydride phase), and 3) thermal desorption spectral behavior [1-23]. Three reasons for lack of characterization are: difficulty achieving proper activity levels for SAV phases with electrolysis, the kinetics for their formation in the bulk is slow resulting in very small volume fractions, and their discovery was fairly recent.

The deuterons within the tubes of δ phase can be regarded (and modeled) as a case of a one dimensional Bravais lattice of ions which has been described in solid state physics texts [27-29]. This paper develops such a model, examines longitudinal lattice vibrations of deuterons along edges of the unit cell, and uses a commercially available solid modeling computer-aided design software package (SolidWorks published by Dassault Systèmes with settings listed in Appendix A) to simulate these vibrations (frequencies, amplitudes and velocities) within the tubes.

2. Analysis and Model Development

A one dimensional row of ions in a monatomic Bravais lattice, after Dean [30] and Ashcraft and Mermin [27], is shown in Fig. 1a. Each ion of mass m is tied to its neighbor with ideal Hookean massless springs with only nearest neighbor forces considered. All springs and ions are connected, so the extreme end springs are viewed as being connected back to the beginning of the string by a loop with a large number of ions with the end spring (on the right) connected to the beginning ion (on left). Alternatively, connectivity is realized by a massless, perfectly rigid bar (Fig. 1a), capable of motion, assuring any motion on either extreme end is replicated at the opposite extreme end, as in the loop version.

With these end conditions, which assure connectivity from ion to ion only, Newton's second law of motion is applied longitudinally to each ion in the string and yields a dispersion relation of lattice waves or phonons [27, 28, 30] relating circular frequency ω (rad/s) for normal modes of vibration to the wave vector q and the ion lattice constant a as:

$$\omega = 2\,\omega_o \sin\,(q \cdot a/2). \qquad (1)$$

Here ω_o is $(k/m)^{1/2}$, the square root of the ratio of the Hookean spring constant k to the mass m of the ion and is considered the fundamental circular frequency (rad/s). This dispersion relation assumes a large number of ions and is suitable for monolithic microstructures, but is untenable in this model where phase boundaries pose different string end conditions, and SAV size is often limited from kinetics and processing conditions. To account for phase boundaries and finite number of ions, end conditions are altered: the extreme right and extreme left springs are fixed to rigid constraints (built in and motionless) as shown in Fig. 1b. Then the exact dispersion relation from Kittle [28] and Torre [29] becomes:

$$\omega = 2\,\omega_o \sin\,(m\pi/2(N+1)) \qquad (2)$$

where N is the total finite integral number of ions in the string. Each ion is numbered as m, so m is integral, $1 \le m \le N$, and called the mode number of the vibration. This relation is exact for all m and N, even if N is small, e.g. 3 to 10, and has the conditions of Fig. 1b with end conditions fixed and excited with a forcing function on one end (see Discussion section for condition of forced vibration at both ends). This is useful since the total number of ions, N^3, in isolated particles of δ phase, and their volume $(N \cdot a)^3$, have been shown to be a very small (e.g. 0.03 %) volume fraction of the bulk [22, 23]. These small particles of δ phase, distributed within the bulk, are consistent with nucleation and growth mechanisms.

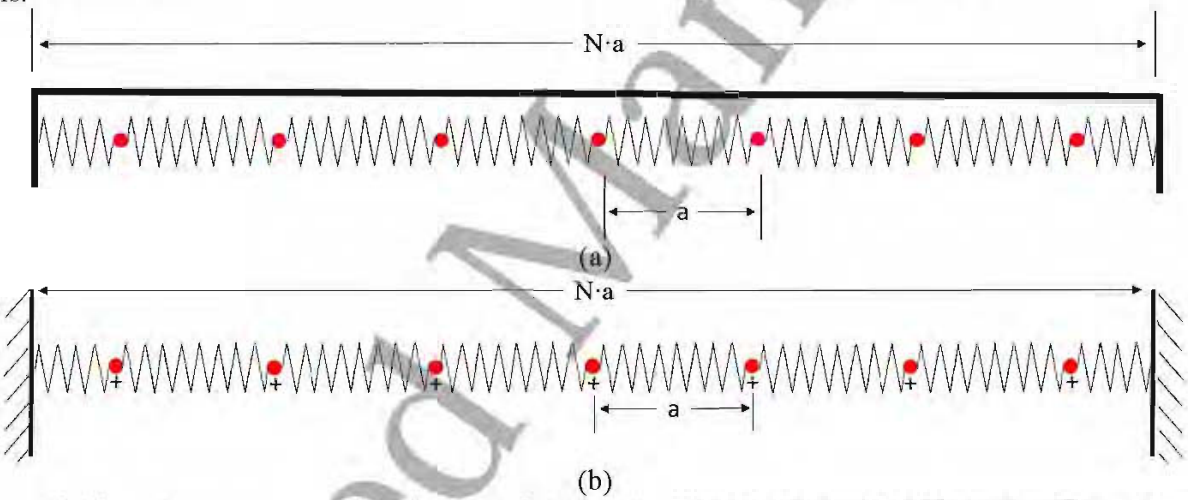

Fig. 1. (a) A model of ions of mass m in a one–Dimensional Bravais Lattice where each ion is tied to its neighbor with an ideal Hookean massless springs with force constant k and only nearest neighbor forces are considered. Here the extreme ends of the springs are connected to a massless and infinitely ridged bar capable of motion, where the motion of one extreme end of the lattice is reproduced at the opposite extreme end of the lattice. Ions have a spacing (lattice constant) of **a**, and the total length of the string of N ions is N·**a**. (b) Here the extreme ends of the springs are fixed, a built-in condition, lending the solution suitable for small finite number N of ions.

Equation (2) is evaluated for each mode m and any N to yield a ratio of normal mode ω to fundamental circular frequency, ω/ω_o. Thus the string has other normal modes, also called natural circular frequencies ω (or frequencies $f = (1/2\pi)\cdot\omega$, in Hz), in addition to the fundamental circular frequency ω_o (or fundamental frequencies $f_o = (1/2\pi)\cdot\omega_o$). Fig. 2 shows eq. (2) solutions of natural frequencies f for selected m modes and N ions. For any N, there are N natural frequencies, one for each m, consistent with string length (N·a). If the string is forced to vibrate longitudinally along its length at one of these natural frequencies, it will resonate with amplitude increasing to large values.

In the case of deuterons in the δ phase, the fundamental frequency $(1/2\pi)\cdot(k/m)^{1/2}$ is its thermal vibration frequency, determined from experimental measurements. Table 1 in the Appendix B lists fundamental thermal vibrational frequencies f_o of isotopes of hydrogen in palladium under various conditions (phases) from the literature as well as the thermal vibration frequency of Pd. These do not account for the string nature, as in this model, but only account for isolated single ions of isotopic hydrogen in their respective lattice positions. The consequences, of this model with string geometry, are extra natural frequencies, from eq. (2) and Fig. 2 in addition to those fundamental ones in Table 1.

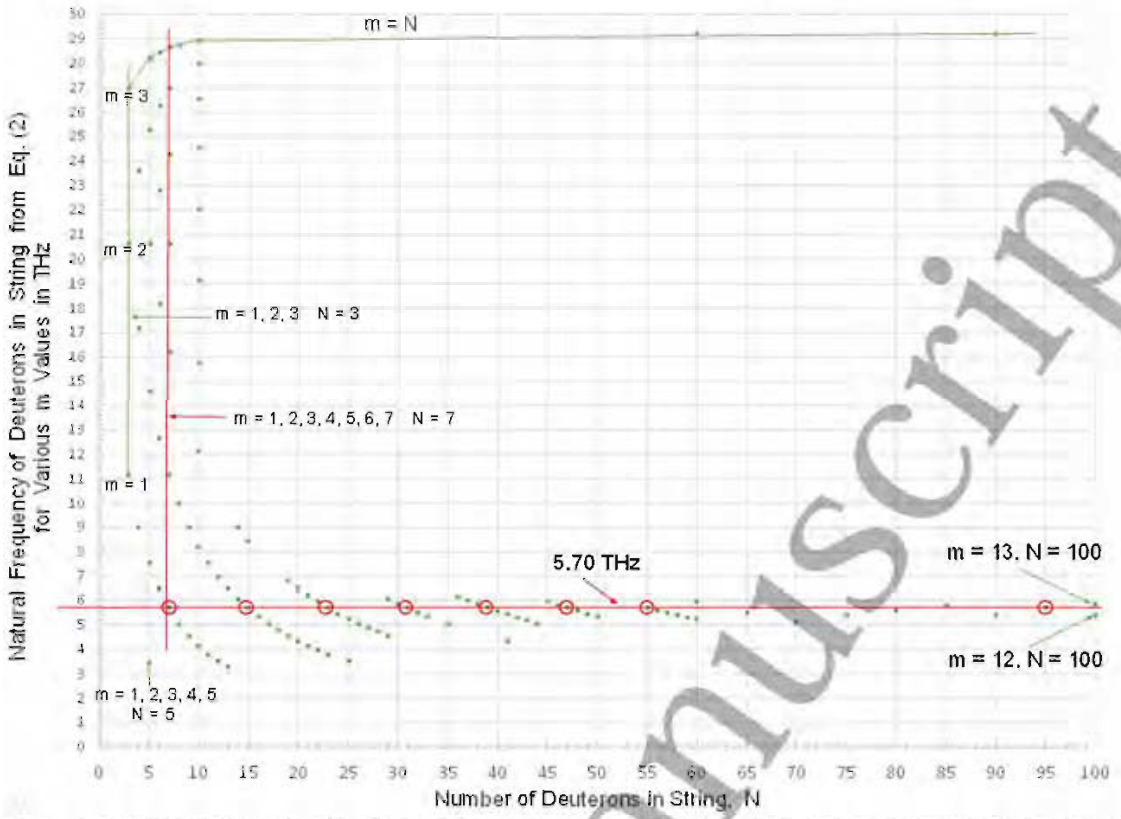

Fig. 2. The values from the model using equation (2) of natural frequencies f (normal modes of longitudinal vibration) of any given length of a string of N ions with m modes of resonances, using $f = (1/2\pi)\cdot\omega$ and $f_o = (1/2\pi)\cdot(k/m)^{1/2}$. Each dot is a normal mode of vibration and possible natural frequency resonance if forced to vibrate at that frequency. The thermal vibration frequency of the Pd lattice is shown at 5.70 THz (see Table 1 in the Appendix B). The dots with circles are driven to resonance by the Pd atom at the end of the string. There are other solutions to equation (2) but only selected most relevant ones are shown near 5.70 THz. The minimum number of ions N to give a match to the frequency of the Pd vibration is N = 7, with other matches at N = 15, 23, 31, 39, 47, 55, 63, 71, 79, 87, 95... etc. indicted with circles.

These strings are a result of the unique lattice geometry of SAV channels in δ phase shown in Fig. 3 where both lattices of beta (β) deuteride of Pd-D and δ of Pd_3VacD_4 are compared. Here a (001) plane is shown with 6 unit cells of δ phase in [100] direction sandwiched between β phase. Repeats of unit cells in [010] and [001] directions are not shown, but the model applies in all 3 orthogonal directions (orthogonal strings of deuterons intersect at corners of each unit cell). The comparison of a string of deuterons in [100] direction of δ phase to the one dimensional Bravais lattice of ions is shown in Fig. 4, and suggests Eq. (2) of the one dimensional Bravais lattice, be used to model δ phase.

The uniqueness of δ phase with ordered Vac^- at corners of unit cells supports this correlation to the one dimensional Bravais lattice of ions, and its description by eq. (2). Density Function Perturbation Theory (DFT) [12, 15-21] shows there is a binding energy between positively charged deuterons and Vac^-, indicating negative charge associated with Vac^-. Pd atoms from β phase fix the end springs because they are 52.8 times more massive and their thermal vibration frequency is lower, but can also exert longitudinal forces on the deuteron string from thermal motion. As Pd atoms vibrate, the deuteron spring compresses and stretches producing Hookean forces on the string equal to displacement (vibration amplitude) times the spring force constant k of the deuteron's spring. In this model, the spring constant for deuteron springs is determined from $f_o = (1/2\pi)\cdot(k/m)^{1/2}$, so $k = m\cdot 4\cdot\pi^2\cdot f_o^2$. Since the fundamental frequency for deuterons in δ phase is f_o = 14.59 THz (Table 1. Appendix B), k = 28.102 N/m, using deuteron mass of 3.344×10^{-27} Kg. From Table 1, the amplitude of vibration of Pd is 0.107 Angstroms (Å) at room temperature. This amplitude (1.07×10^{-11} m) times 28.102 N/m gives a force of 3.01×10^{-10} N exerted on the deuteron string in <100> directions by Pd. Deuterons on perpendicular edges of the unit cell do not have an uninterrupted direct line of sight as they do in the channels and are not considered in this model to result in nearest neighbor forces since they are shielded by the Pd atoms at the center ½,½,0 of the FCC unit cell face. Additional vibration modes arise from the tube geometry, the δ/β phase boundaries, and the negative charge of both Vac^- on each side of the positive deuteron (Figs. 3 and 4). The deuterons have a double attraction to each Vac^- on either side allowing the spring constant to maintain linearity and constancy to high values of deuteron displacement within channels (<100> directions), a main feature of the model. Negative charge in the vicinity of each Vac^- screens positive deuterons approaching from opposite directions (optical mode), allowing closer approach than would be otherwise possible. Without this, spring constant k is variable and depends on the displacement, increasing as two deuterons approach one another near a *neutral* corner vacancy site due to their positively charged nuclei.

Of all the normal modes of vibration (natural frequencies) indicated from eq. (2) and Fig. 2 of deuteron strings in δ phase, many match the forcing vibration of the Pd atom at the end of the δ phase. From Table 1 this frequency for Pd

vibration, when loaded with isotopic hydrogen, is 5.70 THz. It matches values in Fig. 2: the first is at N = 7, m = 1 (exact match), second at N = 15, m = 2 (exact), third exact match at N = 23, m = 3 and forth exact match at N = 31, m = 4. Other exact matches to natural frequency of Pd thermal vibration frequency occur at N and m pairs of: 39 and 5, 47 and 6, 55 and 7, 63 and 8, 71 and 9, 79 and 10, 87 and 11, 95 and 12… etc. This pattern continues to higher values of N and m, repeating every eighth N value. In addition, there are near matches at 14 and 2, 15 and 3, 16 and 2 etc., (from eq. 2 solutions). As N increases the closeness of near matches improves until most of the values of m between the exact matches become near matches. It will be seen in the next section on Simulation why near matches are effectively the same as exact matches: resonance peaks have widths in frequency that include near match values.

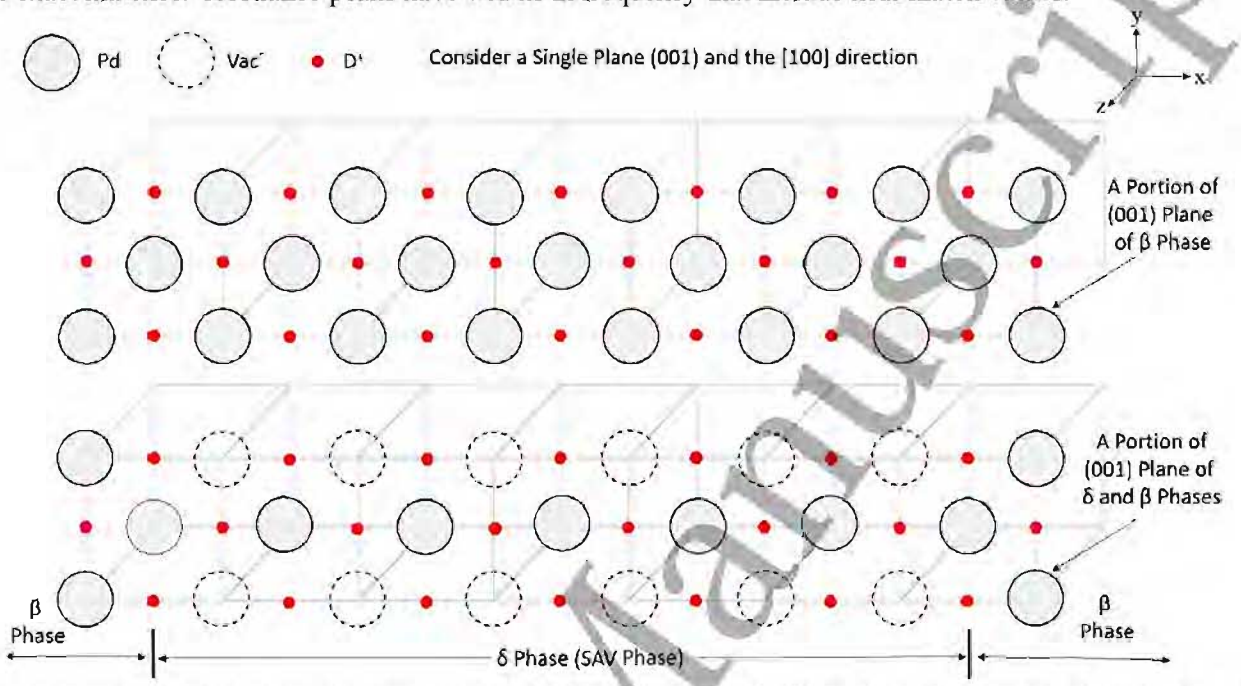

Fig. 3. A comparison of the (001) planes of β phase with a D/Pd ratio of 1.0 (top) to that of a two phase microstructure of δ phase between a matrix phase of β phase (bottom). The large diameter solid atoms are Pd, the vacancies (Vac) are dotted (corner positions in the FCC unit cell) and the red ions are deuterons occupying the octahedral interstitial sites.

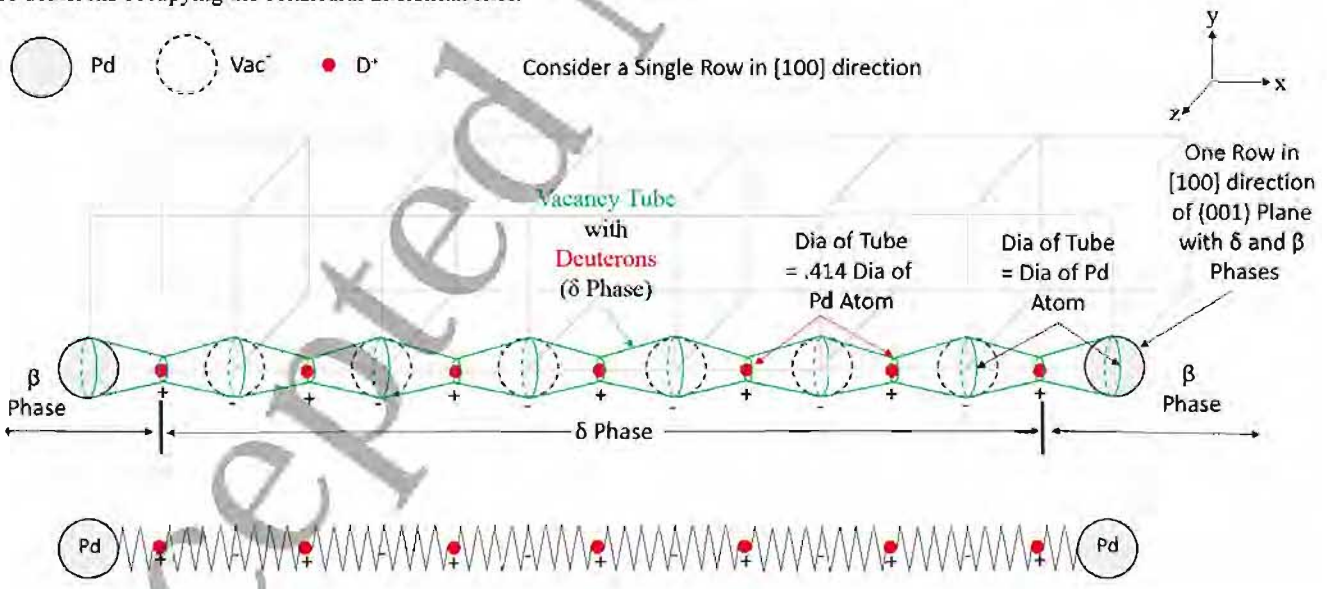

Ball and Spring Model (1 – Dimensional Bravais Lattice) of Deuterons in δ Phase

Fig. 4. A comparison of the [100] direction of the (001) planes of δ phase with deuterons (red) and vacancies (dotted) to that of the one dimensional Bravais lattice of ions connected with springs and with Pd atoms on each extreme end of the string of ions to fix the ends of the extreme springs. The vacancy channel (green tube) is shown with a varying diameter of between .414 and 1.0 of that of the Pd atom diameter (2.75×10^{-10} m). To match the solution of equation (2) one end is fixed by the Pd atom (as in Fig. 1b.) and the other end is forced to vibrate by the Pd atom at that end.

3. Simulation Results with SolidWorks

Since Fig. 2 (eq. 2), shows many matches of natural frequencies to Pd at 5.70 THz, a commercial software package called SolidWorks was utilized to verify if these predictions, with large values of amplitude of vibration of deuterons (resonances), could be simulated. The geometry of a ball (mass) and spring model of Fig. 4 was implemented in the new feature of SolidWorks, *Motion Analysis Simulation*. Models with 1, 3, 7, 10 deuterons, and other values of N in the string, were executed with results shown in Figs. 5 through 8 for 1, 3, 10 and 7 deuterons, respectively. These figures show deuteron vibration resulting from affectedly induced frequencies of vibration of the Pd atom at the end of the string. Fig. 5 represents Pd vibrating at the fundamental frequency of the deuterons: it can only have a resonance if the Pd were to vibrate in the vicinity of 14.59 THz which is not the real value of vibration of Pd (5.70 THz). This simulation with one deuteron was performed as a control simulation, testing effectiveness of SolidWorks to replicate a known natural frequency. Fig. 6 shows three resonances of deuterons at which are also not near that of Pd, but are consistent with the model (no dots in Fig. 2 at N = 3 are close to 5.70 THz). These resonances cannot be triggered by Pd at 5.70 THz. Fig. 7 for a string of 10 deuterons (1000 unit cells of δ) shows 10 resonances ($1 \leq m \leq 10$) none of which perfectly coincide with the thermal vibration of Pd at 5.7 THz: there is an amplitude minimum between that for m = 1 (at 4.153 THz) and m = 2 (at 8.221 THz). However these resonance peaks, due to their widths, almost capture 5.70 THz. As N gets larger the peaks (from eq. 2) near 5.70 THz more nearly overlap the value of 5.70 THz (referred to as "near matches" in the previous section). Fig. 8 shows a resonance peak centered on Pd vibration frequency of 5.70 THz with half max width on both sides of this frequency. This resonance peak coincides exactly with the model prediction (Fig. 2 with N = 7 and m =1), demonstrating Pd atoms do induce resonances at exact matches (and by extension of peak widths, at near matches).

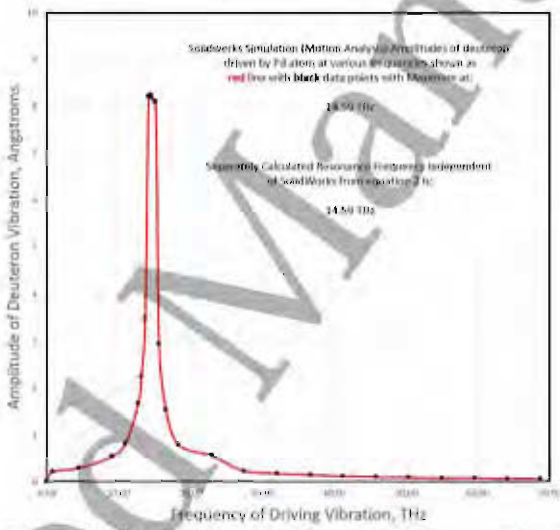

Fig. 5. Amplitude of vibrations of a single deuteron in δ phase driven by Pd atom vibrating at various frequencies f. The peak at 14.59 THz is the fundamental natural resonance frequency and demonstrates the effectiveness of SolidWorks to replicate this normal mode.

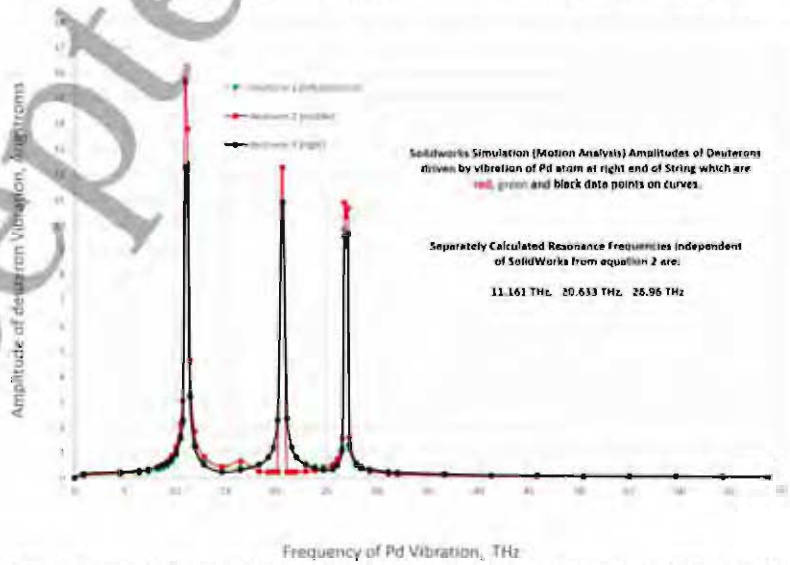

Fig. 6. Amplitude of vibrations of three deuterons in a string on edge of SAV unit cell (δ phase) due to Pd end atom vibration at various frequencies. None of these resonance frequencies match the thermal vibration frequency of Pd at 5.70 THz.

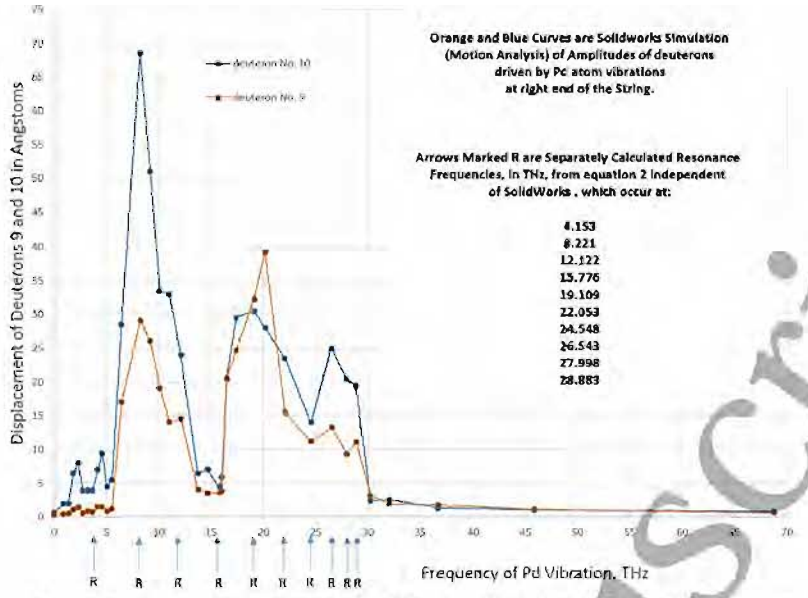

Fig. 7. Amplitude of vibrations of ten deuterons in string on edge of SAV unit cell (δ phase) due to Pd end atom vibration at various frequencies. None of these resonance frequencies exactly match the thermal vibration frequency of Pd at 5.70 THz.

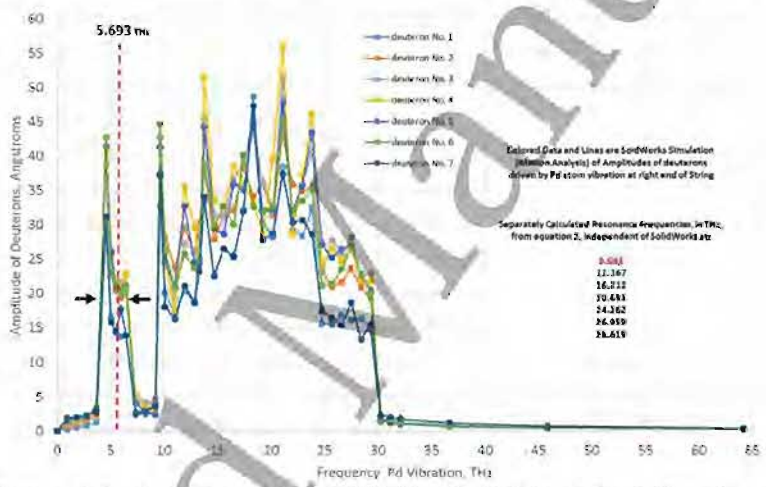

Fig. 8. Amplitude of vibrations of seven deuterons in string on edge of SAV unit cell (δ phase) due to Pd end atom vibration at various frequencies. The first peak (m = 1) at 5.693 THz matches (approximate midpoint of half width) the thermal vibration frequency of Pd (5.70 THz). If peak widths are taken into account, other peaks ($2 \leq m \leq 7$) also match calculated resonance frequencies, but as m increases the peak widths overlap one another.

In addition to amplitude of vibration, the velocity of the deuterons were measured in this study. Fig. 9 (a) shows the velocity of deuteron 7 with respect to deuteron 6. A similar result was obtained for deuteron 3 with respect to deuteron 2. This relative velocity shows the deuterons are effectively vibrating in an optical mode (nearly 180 degrees out of phase) when their relative velocities are near max or min in Fig. 9 (a) (they are separating at positive values and approaching at negative values). They are in acoustical mode when their relative velocities are near zero. Over time they switch back and forth from optical to acoustical mode. From Fig. 9 (a), it can be seen that they approach one another at a velocity of 8.75×10^5 m/s, however it is possible the relative velocity can be as high as twice the absolute velocity (neighboring deuterons completely out of phase), and Fig 9 (b) would indicate this to be as high as 1.16×10^6 m/s or slightly higher since the peak velocity appears to be still increasing at 40 picoseconds.

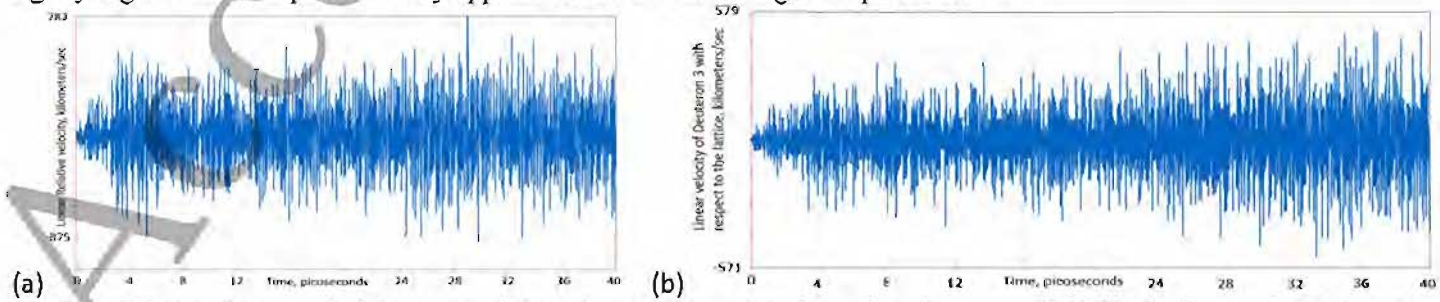

Fig. 9. a) Velocity of deuteron 7 with respect to deuteron 6. A similar result is observed at a frequency of 5.70 THz for deuteron 3 with respect to deuteron 2 and in general any selected set of deuterons at all the seven resonances indicated in Fig. 8. b) Velocity of deuteron 3 with respect to the lattice (absolute velocity). Both a) and b) are for a seven deuteron string due to Pd end atom vibration at a frequency of 21.28 THz.

4. Discussion

This model has several simplifying assumptions that suggest that a more sophisticated approach could reveal additional details. For example, Density Function Perturbation Theory (DFT) would elucidate the shielding ability of the charge of the Vac^- for deuterons approaching one another on opposite sides of the Vac^- and its effect on the spring constant. DFT could also examine how effective the deuterons on mutually perpendicular edges of the unit cell are shielded by both Pd atoms at the center of the face of the unit cell, ½,½,0, of the (001) plane and by the negative charge of the corner Vac^-. Note that the deuteron at the octahedral site at the body center of the unit cell, ½,½,½, is adequately shielded from the deuterons on the octahedral sites on unit cell edges, being completely blocked by Pd atoms in nearest neighbor positions. DFT would handle the dynamics and effectiveness of the negative charge of the Vac^- to shield the interaction of orthogonal strings along mutually perpendicular edges (i.e. [100] and [010], or [100] and [001] or [010] and [001] directions) of each unit cell (i.e. allowing the motion and resonance of mutually perpendicular stings to be independent of one another, or indicate specific interaction). In depth work is underway to address these, but insights gained by this model and simulation may motivate and steer future work on this phenomenon.

The possibility of buckling of the deuteron string in delta phase was compared to buckling in a model of deuterons in a crack [22, 23]. Here, delta phase geometry restrains buckling because: a) positive deuterons move inside a symmetric tube (Fig 4.) having an inside surface with negative charge as a result of the electrons from the surrounding Pd atoms, and this negative charge supports alignment by *pushing* them inward toward the center of the tube, b) deuterons gain considerable velocity, as indicated in Fig 9 (b) as they approach the vacancy site at the corner lattice position, and this momentum discourages transverse motion especially where most needed, near the vacancy, and c) the deuteron's attraction to the negative vacancy site deters transverse motion by *pulling* them inward toward the center of the vacancy. Future DFT calculations may also illuminate these effects.

In this model and in the simulations one end of the string of deuterons is considered fixed while the other end undergoes vibration from the Pd atom. These conditions which fit equation (2) are preserved when both end Pd atoms vibrate if the string has double length ($a\cdot[2\cdot N + 1]$), wherein the central ion is immobile (from symmetry). Simulation runs in SolidWorks with this geometry of double length confirm the central deuteron is indeed motionless even without constraint due to symmetric stimulation (loading). Thus the double length condition for N = 7 becomes two collinear and contiguous stings, each with 7 deuterons, connected by a stationary deuteron in the middle, with the right set of deuterons loaded on its right end and the left set loaded on its left end, thus each set satisfies equation (2) and the associated SolidWorks simulations reported here.

Resonance theory indicates that resonances should occur at very small amplitudes of driver vibrations when dampening is zero, as in this model. Work is underway to address effects of dampening. In this model the force exerted by thermal vibration of Pd on the ends of δ phase (at β phase border) is about 3×10^{-10} N, determined from product of spring constant (28.101×10^{-10} N/m, above) times Pd vibration amplitude. Resonance, solely from thermal vibration, occurs over a range of values used in this study with specific values in Figs. 5 – 8. Values of forces in Figs 5 and 6 were 2×10^{-10} N and Figs. 7 and 8 were 18×10^{-10} N and 20×10^{-10} N respectively, and in all resonances induced solely from thermal motion of Pd atoms as indicated in Fig. 2 at circled dots such as N = 7, m = 1 etc. Acoustic phonons from the Pd lattice feed the necessary energy for the mixed acoustic and optic modes of deuterons leading to these resonances.

5. Conclusions

This model and simulation suggest SAV δ phase crystallography offers a unique geometry for vibrations of deuterons. The results suggest that as the size of δ phase $(N\cdot a_s)^3$ increases, the opportunity for high amplitude vibrations of deuterons increases because of near matches (overlapping resonance peak widths). As the temperature of the Pd host increases, the amplitude of Pd vibration increases, making the possibility of resonance more likely due to a stronger driving force. SolidWorks simulations confirm predictions in the one dimensional Bravais lattice model, validating cases with, and cases that lack, resonance from thermal vibration of Pd atoms.

6. Appendix A: SolidWorks Reference Information

SolidWorks version 2018 was used with scale factors of: distance = 10^7, mass = 2.990430×10^{26}, force = 10^{10}, spring constant = 10^3, frequency = 1.09084×10^{-12}. *Motion Analysis Simulation* settings were: accuracy = .00000001, frames/s = 300, resolution = 50%, and computational times = 5 to 40 s with personal computer real run times lasting about 2 hours for each individual simulation condition.

7. Appendix B: Frequency of Vibration of Isotopic Hydrogen and Palladium under Various Conditions

Table 1. lists fundamental frequency f_o of isotopes of hydrogen (H and D) and palladium (Pd) in various phases. Both Pd-H and Pd-D exist as α, β, δ, and δ' with a range of H/Pd or D/Pd ratios (x values). The solid, liquid and gas phases are listed for comparison and completeness. Both H and D have different values of f_o depending if the hydride PdH_x or deuteride PdD_x is α (low x) or β (x ≥ .63) or δ (x = 1.33, Pd_3VacA_4, where A = H or D in octahedral sites) or δ' (x = 1.33, Pd_3VacA_4, with A in tetrahedral sites). Since suitable amount of data is available from the literature in most cases, averages within a given data set are used in the model and simulations of this paper and listed in Table 1. For example using average values, the ratio of the f_o of β_H/β_D = 1.51 and f_o of α_H/α_D = 1.43 compared to the inverse mass ratio 1.41. The ratio for f_o of δ_H/δ_D is 1.51 (because of reason give below). The f_o of H in δ and δ' are reported in reference 15 giving f_o of δ_H/β_H = 1.57, however f_o of D in δ and δ' are not reported in reference 15. This same ratio (1.57) was used to set δ_D/β_D at 1.57, since the f_o of δ_H/δ_D is assumed to be better represented by f_o of β_H/β_D than by f_o of α_H/α_D, because both β and δ have high x values). Thus the first two entries in the Table 1 are from values from reference 15 and the use of this ratio (1.57) from the observations of the present work (including all the data from Table 1 taken as a whole).

Table 1. Frequency of Vibration f of Isotopic Hydrogen (H or D) and Palladium (Pd) under Various Conditions

Element or Isotope and Its Arrangement or State	Frequency f_o (THz)	Amplitude of Vibration (Angstroms)	PdA_x or Pd_3VacA_4 (A = H or D); Phase = α, β, δ_2 or δ' ; x = A/Pd	Temperature (°K); (P = pressure, GPa)	Reference
D in δ_D Phase (Pd_3VacD_4)	**14.59**		δ, x = 1.33	295	15 & This
D in δ'_D Phase (Pd_3VacD_4)	27.86		δ', x = 1.33	295	15 & work
D in Pd at Octahedral sites	9.52		β, x = .63	295	31 (Fig.3)
(PdD_x Phase)	9.00		β, x = ~.9	295	32
	9.50		β, x = .63	295	33
	9.16		β, x = .63	295	34
	9.21		β, x = .75	295	34
	9.41		β, x = .90	295	34
	9.19	.161	β, x = .63	80	35
	9.60		β, x = .75	<50 and 84	36
	9.60		β, x = .75	20 and 78	37
	8.95		β, x = ~1.0	5	38
Average β_D = 9.30 THz	9.15		β, x = .78	75-85	39
	11.61	.122	α, x = .002	295	40
Average α_D = 11.43 THz	11.24		α, x = .014	295	33
H in δ_H Phase (Pd_3VacH_4)	22.0		δ, x = 1.33	295	15
H in δ'_H Phase (Pd_3VacH_4)	42.0		δ', x = 1.33	295	15
H in Pd at Octahedral sites	13.54	.24 in [100] direction	β, x = .63	295	41
(PdH_x Phase)	13.99		β, x = .63	295	31
	13.78		β	295	42
	14.24		β, x = .63	295	33
	13.90		β, x =.70, .85, .93	80 and 100	43
	14.85		low T. β x = .0011	5	44
	13.36		β, x = .63	80	45
	14.02		β, x = .70	70	46
	14.15		β, x = .75	<50 and 84	36
	14.17		β, x = .63	4	47
Average β_H = 14.02 THz	14.27		low T. β x = .0008	4	47
		.30 in [100] direction	α, x = .03	623	48
	16.44		α, x = .015	295	47
	15.96		α, x = .0008	295	47
	16.26	.175	α, x = .002	295	40
	16.68		α, .002 ≤ x ≤ .014	295	33
	16.49		α, x = .0011	300	44
Average α_H = 16.38 THz	16.44		α, .05 ≤ x ≤ .091	5	38
Pd lattice atoms in PdA_x	5.50		β, x = .63 (A = D)	295	31
(A = H or D)	6.25	.100	β, x = .63 (A = H)	295	41
	5.37		β, x = .63-.90 (A = D)	295	34
		.113	α, x = .007 (A = H)	295	49
Average = 5.70 THz		**.107** (average)			
Pd lattice atoms *without* H or D (pure Pd)	6.78	.10	x = 0	300	31
		.131	x = 0	295	49
Average = 6.74 THz	6.70		x = 0	296	50, 51
For Comparison, Reference Frequencies (THz) for Solid, Liquid, and Gas Hydrogen Isotopes					
D_2 Solid	89.3			300 (P = 150 GPa)	52
Solid	89.5			300 (P = 303 GPa)	53, 54, 55
Liquid	89.6			38	54
Gas	89.7			295	54, 56
H_2 Solid	122			300 (P = 150 GPa)	52
Solid	124			13	57
Liquid	124			14	57
Gas	125			295	54, 56

5. References

[1] Y. Fukai and N. Okuma, Evidence of copious vacancy formation in Ni and Pd under a high hydrogen pressure, *Jpn. J. Appl. Phys.* **32** (1993) 1256.

[2] W. A. Oates and H. Wenzl, On the copious formation of vacancies in metals, *Scripta Met. et Mat.* **30** (1994) 851–854.

[3] W. A. Oates and H.Wenzl, On the formation and ordering of superabundant vacancies in palladium due to hydrogen absorption, *Scripta Met. et Mat.* **33** (2) (1995) 185–193.

[4] Y. Fukai, *The Metal–Hydrogen System: Basic Bulk Properties*, 2nd Edn., Springer, Berlin (2005).

[5] Y. Fukai, Superabundant vacancies formed in metal–hydrogen alloys, *Physica Scripta* 2003 No. T103 (2002) 11.

[6] V. F. Degtyareva, Electronic origin of superabundant vacancies in Pd hydride under high hydrogen pressures, Presented on the Conference on Hydrogen Materials Science (ICHMS), Yalta, Ukraine, 25–31 August (2009): http://arxiv.org/pdf/1001.1525.pdf , accessed 25 November 2018.

[7] D. Tanguy and M. Mareschal, Superabundant vacancies in a metal–hydrogen system: Monte Carlo simulations, *Phys. Rev.* B **72** (17) (2005) 174116.

[8] Y. Fukai, Hydrogen-induced superabundant vacancies in metals: implication for electrodeposition, A. Ochsner, G. E. Murch and J. M. O\Q. Delgado (Eds.), *Defect and Diffusion Form* **312–315** (2011) 1106–1115.

[9] D. S. dos Santos, S. Miraglia and D. Fruchart, A high pressure investigation of Pd and the Pd–H system, *J. Alloys Compd.* **291** (1999) L1– L5.

[10] Y. Fukai and N. Okuma, Formation of superabundant vacancies in Pd hydride under high hydrogen pressures, *Phys. Rev. Lett.* **73** (12) (1994) 1640–1643.

[11] Y. Fukada, T. Hioki and T. Motohiro, Multiple phase separation of super-abundant-vacancies in Pd hydrides by all solid-state electrolysis in moderate temperatures around 300 C, *J. Alloys Compd.* **688** (2016) 404–412.

[12] C. Zhang and Ali Alavi, First-principles study of superabundant vacancy formation in metal hydrides, *J. Am. Chem. Soc.* **127** (2005) 9808–9817.

[13] Y. Fukai, M. Mizutani, S. Yokota, M. Kanazawa, Y. Miura and T. Watanabe, Superabundant vacancy–hydrogen clusters in electrodeposited Ni and Cu, *J. Alloys Compd.* **356–357** (2003) 270.

[14] Y. Fukai, Formation of superabundant vacancies in M–H alloys and some of its consequences: a review, *J. Alloys Compd.* **356–357** (2003) 263–269.

[15] L. E. Isaeva, D.I. Bazhanov, Eyvas Isaev, S.V. Eremeev, S.E. Kulkova and Igor Abrikosov, Dynamic stability of palladium hydride: an ab initio study, *Int. J. Hydrogen Energy* **36** (1) (2011) 1254–1258.

[16] Y. Fukai and H. Sugimoto, Formation mechanism of defect metal hydrides containing superabundant vacancies, *J. Phys. Condensed Matter* **19** (2007) 436201.

[17] H. Sugimoto and Y. Fukai, Migration mechanism in defect metal hydrides containing superabundant vacancies, *Diffusionfundamentals.org* 11 (2009) 102, pp. 1–2.

[18] L. Bukonte, T. Ahlgren and K. Heinola, Thermodynamics of impurity-enhanced vacancy formation in metals, *J. Appl. Phys.* **121** (2017) 045102-1 to -11. https://doi.org/10.1063/1.4974530.

[19] Y. Fukai and H. Sugimoto, The defect structure with superabundant vacancies to be formed from FCC binary metal hydrides: Experiments and simulations, *J. Alloys Compd.* **446, 447** (2007) 474–478.

[20] R. Nazarov, T. Hickel and J. Neugebauer, Ab Initio study of H-vacancy interactions in FCC metals: implications for the formation of superabundant vacancies, *Phys. Rev.* B **89** (2014) 144108.

[21] Y. Fukai, Y. Kurokawa and H. Hiraoka, Superabundant vacancy formation and its consequences in metal hydrogen alloys, *J. Jpn. Inst. Met.* **61** (1997) 663–670 (in Japanese).

[22] M. R. Staker, Coupled calorimetry and resistivity measurements, in conjunction with an emended and more complete phase diagram of the palladium - isotopic hydrogen system, J. Cond. Matter Nucl. Sci. **29** (2019) 129-168.

[23] M. R. Staker, Estimating volume fractions of superabundant vacancy phases and their potential roles in low energy nuclear reactions and high conductivity in the palladium – isotopic hydrogen system, Mat. Sci. Eng. B (2020) in press.

[24] M. P. Pitt and E. MacA. Gray, tetrahedral occupancy in the Pd–D system observed by *in situ* neutron powder diffraction, *Europhys. Lett.* **64** (3) (2003) 344–350.

[25] G. A. Ferguson Jr., A.I. Schindler, T. Tanaka and T. Morita, Neutron diffraction study of temperature-dependent properties of palladium containing absorbed hydrogen, *Phys. Rev.* **137** (2A) (1965) 483.

[26] K. G. McLennan, E. MacA. Gray and J. F. Dobson, Deuterium occupation of tetrahedral sites in palladium, Phys. Rev. B78 (2008) 014104.

[27] N. W. Ashcraft and N. D. Mermin, Solid State Physics, Harcourt College Publishers, Orlando, FL (1976) p.432.

[28] Charles Kittel, Introduction to Solid State Physics, 8th Ed., John Wiley and Sons, Hoboken, NJ (2005) pp. 108-110.

[29] Charles G. Torre, Foundations of Wave Phenomena: Complete Version (8.3) , *Department of Physics, Utah State University*, December 2016, pp. 29-31. https://digitalcommons.usu.edu/foundation_wave/ , accessed 17 Jan 2020.

[30] P. Dean, Atomic vibrations in solids, J. Institute of Maths Applics (*Institute of Mathematics and its Applications Journal of Applied Mathematics*) **3** (1967) 98-165. https://doi.org/10.1093/imamat/3.1.98
[31] J. M. Rowe, J. J. Rush, H. G. Smith, M. Mostoller, and H. E. Flotow, Lattice Dynamics of a Single Crystal of $PdD_{.63}$, Physical Review Letters **33** (1974) 1297-1300.
[32] M. A. Kuzovnikov, Vibrational Properties of H Impurity in High-Pressure Palladium Deuteride, Institute Solid State Phys., Russian Acad. Sci., Chernogolovka, kuz@issp.ac.ru, http://www.issp.ac.ru/lhpp/PapersKuzovnikov/Kuz4.pdf
[33] J. J. Rush, J. M. Rowe, and D. Richter, Direct Determination of the Anharmonic Vibrational Potential for H in Pd, Zeitschrift für Physik B Condensed Matter **55** Issue 4 (1984) 283-286.
[34] L. E. Sansores, J. Tagueiia-Martinez and, R. A. Tahir-Kheli, Lattice Dynamics of PdD, and PdH, J. Phys. C: Solid State Phys **15** (1982) 6907-6917.
[35] C. J. Glinka, J. M. Rowe, J. J. Rush, A. Rahman, S. K. Sinha, and H. E. Flotow, Inelastic-neutron-scattering Line Shapes in PdD.63, Physical Review B **17** (1978) 488-493.
[36] R. Sherman, H. K. Birnbaum, J. A. Holy and M. V. Klein, Raman Studies of Hydrogen Vibrational Modes in Palladium, Phys. Lett. **62A** (1977) 353-355.
[37] Robert Sherman, Raman Studies of Hydrogen Vibrational Modes in Palladium, Master of Science Thesis in Metallurgical Engineering, University of Illinois at Urbana-Champaign (1978).
[38] V. E. Antonov, A. I. Davydov, V. K. Fedotov, A. S. Ivanov, A. I. Kolesnikov, and M. A. Kuzovnikov, Neutron Spectr. of H Impurities in PdD Covibratins of the H and D Atoms, Physical Review B **80** (2009)134302-1 to 134302-7.
[39] Q. Blaschko, R. Klemencic, and P. Weinzier, L. Pintschovius, Lattice dynamics of β-$PdD_{.78}$ at 85 K and Ordering Effects at 75 K, Physical Review B **24**, No. 3 (1981) 1552-1555.
[40] W. Drexel, A. Murani, D. Tocchetti, W. Kley, I. Sosnowska, and D. K. Ross, The Motions of Hydrogen Impurities in Alpha-Palladium-Hydride, J. Physics and Chemistry of Solids **37**, Issue 12 (1976) 1135-1139.
[41] J. Bergsma and J. A. Goedkoop, Thermal Motion In Palladium Hydride Studied By Means of Elastic and Inelastic Scattering of Neutrons, Physica **26**, Issue 9 (1960) 744-750.
[42] M. R. Chowdhury and D. K. Ross, A neutron scattering study of the vibrational modes of hydrogen in the β-phases of Pd-H, Pd-10Ag-H and Pd-20Ag-H, Solid State Communications **13**, Issue 2 (1973) 229-234.
[43] D. K. Ross, P. F. Martin, N. A. Oates, and R. Khoda Bakhsh, Inelastic Neutron Scattering Measurements of Optical Vibration Frequency Distributions in Hydrogen-Metal Systems, Zeitschrift fur Physikalische Chemie Neue Folge, Bd **114** (1979) 221-230. Published Online: 2011-08-30 DOI: https://doi.org/10.1524/zpch.1979.114.114.221.
[44] Tai-NiYang, Trapped Hydrogen Vibrational Density of States Measurement Using IINS $PdH_{0.0011}$ at 5 K and 300 K with Incident Neutron Energy of 250 Mev, Master of Science Thesis, University of Illinois at Urbana-Champaign (2013).
[45] A. Rahman, K. Skold, C. Pelizari, S. K. Sinha, and H.E. Flotow, Photon Spectra of Non-stoichiometric Pd Hydrides, Phys. Rev. B **14** (1976) 3630-3634.
[46] D. G. Hunt and D. K. Ross, Optical Vibrations of H in Metals, J. of the Less Common Metals 49 (1976) 169-191.
[47] Brent J. Heuser, T. J. Udovic, Hyunsu Ju, Vibrational Density of States Measurement of Hydrogen Trapped at Dislocations in Deformed $PdH_{0.0008}$, Physical Review B **78** (2008) 214101.
[48] J. M. Rowe, J. J. Rush, L. A. de Graaf, and G. A. Ferguson, Neutron Quasielastic Scattering Study of Hydrogen Diffusion in a Single Crystal of Palladium, Physical Review Letters **29**, Number 18 (1972) 1250-1253.
[49] E. A. Owen and E. W. Evans, The Effect of The Occlusion of Hydrogen on the Characteristic Temperature of Palladium and the Vibration Amplitudes of Its Atoms, British Journal of Applied Physics **18**, Number 5 (1967) 605-610.
[50] A. P. Miiller and B. N. Brockhouse, Anomalous Behavior of the Lattice Vibrations and the Electronic Specific Heat of Palladium, Phys. Rev. Lett. **20** (1968) 798-801.
[51] A. P. Miiller and B. N. Brockhouse, Crystal Dynamics and Electronic Specific Heats of Palladium and Copper Canadian Journal of Physics **49** (1971) 704-723.
[52] Philip Dalladay-Simpson, Ross T. Howie & Eugene Gregoryanz, Evidence for a New Phase of Dense Hydrogen Above 325 Gigapascals, Nature **529** (2016) 63–67. https://www.nature.com/articles/nature16164?proof=trueIn#f3
[53] Chang-sheng Zha, R. E. Cohena, Ho-kwang Maoa, and Russell J. Hemley, Raman Measurements of Phase Transitions in Dense Solid Hydrogen and Deuterium to 325 Gpa, Proceedings of the National Academy of Science of the United States of America (PNAS) Vol. **111**, No.13 (2014) 4792-4797. www.pnas.org/cgi/doi/10.1073/pnas.1402737111.
[54] Andrea Centrone, Diana Y. Siberio-Perez, Andrew R. Millward, Omar M. Yaghi, Adam J. Matzger, Giuseppe Zerbi, Raman Spectra of H and D Adsorbed on a Meta-Organic Framework, Chem. Phys. Lett. 411 (2005) 516-519.
[55] B.P. Stoicheff, High Res. Raman Spectroscopy Gases: IX. Spectra H_2, HD, and D_2, Can. J. Phys. **35** (1957) 730-741.
[56] G. D. Dickenson, M. L. Niu, E. J. Salumbides, J. Komasa, K. S. E. Eikema, K. Pachucki, and W. Ubachs, Fundamental Vibration of Molecular Hydrogen, Physical Review Letters PRL **110**, (2013) 193601.
[57] Elizabeth J. Allin, T. Feldman, *and* H. L. Welsh, Raman Spectra of Liquid and Solid Hydrogen, Journal of Chem ical Physics **24**, Issue 5 (1956) 10.1063/1.1742711. https://aip.scitation.org/doi/10.1063/1.1742711